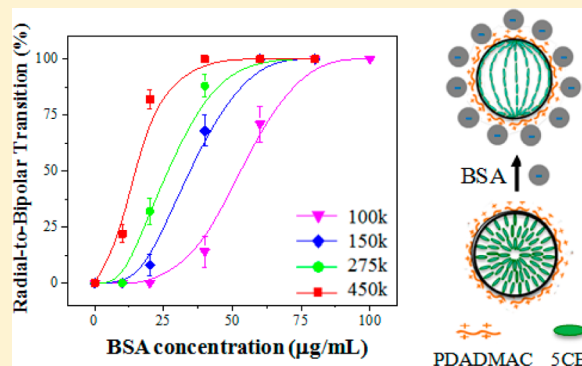


Protein-Induced Configuration Transitions of Polyelectrolyte-Modified Liquid Crystal Droplets

Tanmay Bera, Jinan Deng, and Jiyu Fang*

Department of Materials Science and Engineering, University of Central Florida, Orlando, Florida 32826, United States

ABSTRACT: Liquid crystal (LC) droplets dispersed in aqueous solution have emerged as an optical probe for sensing the adsorption and interaction of biological species at the LC/aqueous interface. In this paper, we modify the surface of 4-*n*-pentyl-4'-cyanobiphenyl (5CB) LC droplets by the adsorption of positively charged poly(diallyldimethylammonium chloride) (PDADMAC) and poly(ethylenimine) (PEI) with different molecular weights at the 5CB/water interface. The PDADMAC and PEI-modified 5CB droplets show a radial director configuration in aqueous solution with salt concentrations above 150 mM. The adsorption of negatively charged bovine serum albumin (BSA) on the positively charged PDADMAC and PEI-modified 5CB droplets through electrostatic interaction can induce the radial-to-bipolar configuration transition of the 5CB inside the droplets. We find that the concentration of BSA required to induce the configuration transition increases linearly with the decrease of the molecular weight of PDAMAC and PEI. Our results highlight the capability of the director configuration of LC droplets as an optical probe for sensing the interaction between proteins and polyelectrolytes at the LC/aqueous interface.



1. INTRODUCTION

Polyelectrolyte–protein systems have received considerable attention because of their applications in protein separations,^{1,2} drug delivery,^{3,4} and biosensors.^{5–7} Efforts have been made in studying the interaction of proteins and polyelectrolytes in solution and at interfaces in order to design polyelectrolyte–protein systems for specific applications.^{8–11} Current methods, which are commonly used for detecting the adsorption of proteins on polyelectrolyte layers, are surface plasmon resonance,^{12,13} quartz crystal microbalance,^{14–16} and confocal fluorescence microscopy.^{17–19}

Liquid crystal (LC) droplets dispersed in aqueous solution with large surface areas, rich phases, and tunable optical properties have recently emerged as a simple optical probe to detect the adsorption and interaction of biological species at the LC/aqueous interface.²⁰ It is known that the director configuration of LC droplets reflects the balance between the elasticity and the surface anchoring of the LC inside the droplets.²¹ The adsorption and interaction of biological species at the LC/aqueous interface may disrupt the balance, inducing the configuration transition of the LC inside the droplets, which allows these events occurring at the interface to be observed with the bare-eye under a polarizing optical microscope without needing expensive and complex detection systems for signal transductions. Recently, there is increased interest in chemically modifying the surface of LC droplets dispersed in aqueous solution by the adsorption of polymers at the LC/aqueous interface for sensor applications.^{22–32}

Polyelectrolytes are a polymer whose repeating units bear electrolyte groups. The dissociation of the electrolyte groups in aqueous solution makes the polymer charged. It has been

shown that the adsorption of negatively charged poly(styrenesulfonate sodium) (PSS) at the LC/aqueous interface can stabilize the LC droplets formed in aqueous solution and induce a bipolar director configuration of the LC inside the droplets.^{23,25} The PSS-modified LC droplets can be further modified by the layer-by-layer assembly of polyelectrolytes. In this paper, positively charged poly(diallyldimethylammonium chloride) (PDADMAC) and poly(ethylenimine) (PEI) with different molecular weights are used to modify the surface of 4-*n*-pentyl-4'-cyanobiphenyl (5CB) LC droplets in aqueous solution by their adsorption at the LC/aqueous interface. We find that the bipolar configuration of the 5CB inside the PDADMAC and PEI-modified droplets changes to a radial configuration by increasing the concentration of sodium chloride (NaCl) in aqueous solution. The positively charged PDADMAC and PEI-modified 5CB droplets with the radial configuration in NaCl solution are used to detect the adsorption of negatively charged proteins, in which the director configuration of the 5CB inside the droplets is used as an optical probe. As a proof-of-concept, negatively charged bovine serum albumin (BSA) is chosen because it is an abundant protein in nature. We find that the adsorption of BSA on PDADMAC and PEI modified-5CB droplets through electrostatic interaction induces a radial-to-bipolar configuration transition of the 5CB inside the droplets. The concentration of BSA required to induce the configuration transition increases

Received: February 13, 2014

Revised: April 10, 2014

Published: April 11, 2014

linearly with the decrease of the molecular weight of PDADMAC and PEI, respectively.

EXPERIMENTAL METHODS

Materials. Sodium chloride (NaCl), sodium hydroxide (NaOH), and phosphate buffer saline (PBS) were from Sigma-Aldrich. Poly(ethylenimine) (PEI) with average molecular weights of ~ 1.7 kDa, ~ 10 kDa, ~ 70 kDa, and ~ 750 kDa and poly(diallyldimethylammonium chloride) (PDADMAC) with average molecular weights of ~ 100 kDa, ~ 150 kDa, ~ 275 kDa, and ~ 450 kDa were purchased from Alfa-Aesar. Bovine serum albumin (BSA), fluorescein conjugated BSA (FITC-BSA), and 4-*n*-pentyl-4'-cyanobiphenyl (SCB) were purchased from Sigma-Aldrich. Tobacco mosaic virus (TMV) was from the American Type Culture Collection. Water used in experiments was purified with the Easy-Pure II system ($18\text{ M}\Omega\text{ cm}$, pH 5.4).

Methods. To modify the surface of SCB droplets dispersed in aqueous solution with PDADMAC or PEI, $10\text{ }\mu\text{L}$ of SCB was added in 10 mL deionized water containing 20 mg/mL PDADMAC or PEI at pH 5.4 in a glass vial. The mixed solution was sonicated for 15 min. The resultant PDADMAC and PEI-modified SCB droplets were washed with deionized water through centrifugation to remove excess PDADMAC and PEI, respectively. The PDADMAC and PEI-modified SCB droplets were then analyzed with an optical microscope to estimate their concentrations, in which a drop ($2\text{ }\mu\text{L}$) of SCB droplet solution was placed between two cover glass slides, and a large number of optical microscopy images were captured to represent the whole sample area. The number of the droplets confined by the two cover glass slides was carefully counted from the optical microscopy images and then used to calculate the concentration of the modified SCB droplets in the initial solution. Finally, the PDADMAC and PEI-modified SCB droplets were dispersed in 150 mM NaCl solution in the pH range from 7.4 to 8.7 or PBS solution for the study of the interaction of BSA with PEI or PDADMAC at the surface of the SCB droplets, in which the concentration of the modified-SCB droplets was kept at $\sim 4.2 \times 10^6$ droplets per mL.

Characterizations. The director configuration of the SCB inside the droplets was analyzed with a polarized optical microscope (Olympus BX40) in transmission mode. A large number of polarized optical microscopy images was captured and then analyzed to estimate the percentage of the SCB droplets, which had undergone the director configuration transition after the adsorption of BSA. ζ -Potential measurements were carried out using Zetasizer Nano ZS90 (Malvern Instruments Inc.) at room temperature under a cell-driven voltage of 30 V , in which $750\text{ }\mu\text{L}$ of SCB droplet solution was added into the zeta potential cuvettes and the average of 10 scans was taken for each measurements. The size of SCB droplets in aqueous solution were measured with dynamic light scattering (PD 2000DLS). Confocal fluorescence images were acquired with a Zeiss AxioScope-2 MOT microscope with an argon–Krypton laser.

RESULTS AND DISCUSSION

The chemical structures of PDADMAC and PEI are shown in Figure 1. Both of them are positively charged polyelectrolytes. The SCB droplets are formed by sonication in deionized water at pH 5.4 in the presence of PDADMAC and PEI, respectively. The adsorption of positively charged PDADMAC or PEI at the

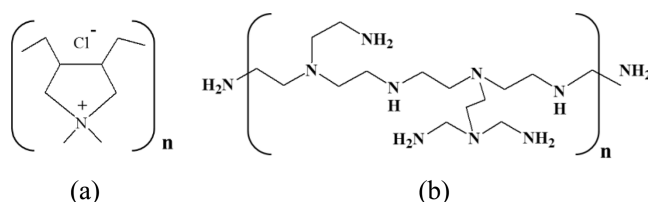


Figure 1. Chemical structures of poly(diallyldimethylammonium chloride) (PDADMAC) (a) and poly(ethylenimine) (PEI) (b).

SCB/water interface stabilizes the SCB droplets in deionized water. The average diameter is $\sim 0.82\text{ }\mu\text{m}$ for PEI-modified SCB droplets and $\sim 0.77\text{ }\mu\text{m}$ for PDADMAC-modified SCB droplets, respectively. The ζ -potential is 43.6 mV for 750 kDa PEI-modified SCB droplets and 45.2 mV for 450 kDa PDADMAC-modified SCB droplets, respectively. Figure 2a shows a polarizing optical microscopy image of PDADMAC-modified SCB droplets in deionized water at pH 5.4. All the PDADMAC-modified SCB droplets are found to have a bipolar configuration, which is independent of the molecular weight of PDADMAC. When the concentration of NaCl added in droplet solution reaches 150 mM , the director of the SCB inside the PDADMAC-modified droplets transits to a radial configuration (Figure 2c). The PEI-modified SCB droplets also show the bipolar-to-radial transition in aqueous solution after the addition of 150 mM NaCl. The configuration transition of PDADMAC and PEI-modified SCB droplets is a result of the formation of an electrical double-layer at the SCB/aqueous interface, which is able to induce a homeotropic anchoring.³³

Then, we adjusted the pH of droplet solution to 7.4 for the study of the binding of BSA on the PDADMAC- and PEI-modified SCB droplets via electrostatic interaction. The positively charged PDADMAC-modified SCB droplets remain a radial configuration in aqueous solution with 150 mM NaCl at pH 7.4 (Figure 3a). After the addition of 2 mg/mL BSA solution for 30 min, the ζ -potential of 450 kDa PDADMAC modified-SCB droplets drops from 45.2 mV to 8.3 mV , suggesting the adsorption of negatively charged BSA on the PDADMAC-modified SCB droplets. Figure 3b shows a polarizing optical microscopy image of 450 kDa PDADMAC-modified SCB droplets after the adsorption of BSA. Interestingly, the SCB inside the PDADMAC-modified SCB droplets transits to a bipolar configuration. If the concentration of NaCl in the droplet solution reaches to $\sim 1.5\text{ M}$, we find that there is no adsorption of BSA on PDADMAC-modified SCB droplets due to charge screening, suggesting that electrostatic interaction is a driving force for the adsorption of BSA. Confocal fluorescent microscopy further confirms that the adsorption of BSA on the PDADMAC-modified SCB droplets is responsible for the radial-to-bipolar configuration transition. In our experiments, 2 mg/mL FITC-labeled BSA was added into PDADMAC-modified SCB droplet solution containing 150 mM NaCl at pH 7.4. After 30 min incubation, the bright-field microscopy image shown in Figure 3c reveals the formation of bipolar SCB droplets (Figure 3c), in which the two defect points of the bipolar SCB droplets are visible. As can be seen from the confocal fluorescent microscopy image shown in Figure 3d, the surface of the bipolar SCB droplets shows strong fluorescence, confirming the adsorption of FITC-BSA on PDADMAC-modified SCB droplets. In addition, the confocal fluorescent microscopy image also shows that the fluorescence intensity from the two defect points of the bipolar SCB droplet are stronger than that of the rest part of the

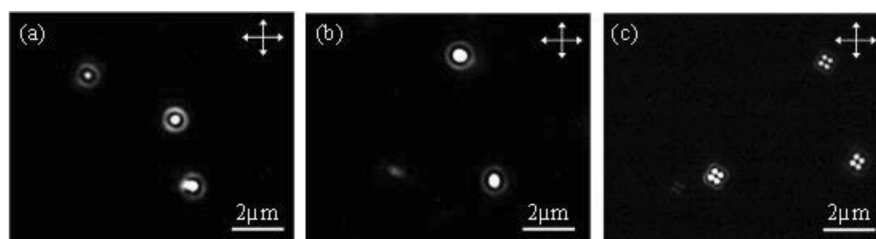


Figure 2. Polarizing optical microscopy images of PDADMAC-modified 5CB droplets in aqueous solution with 0.0 mM (a), 100 mM (b) and 150 mM (c) NaCl at pH 5.4. 450 kDa PDADMAC was used in the modification of 5CB droplets. The direction of the polarizer and analyzer is indicated by white arrows.

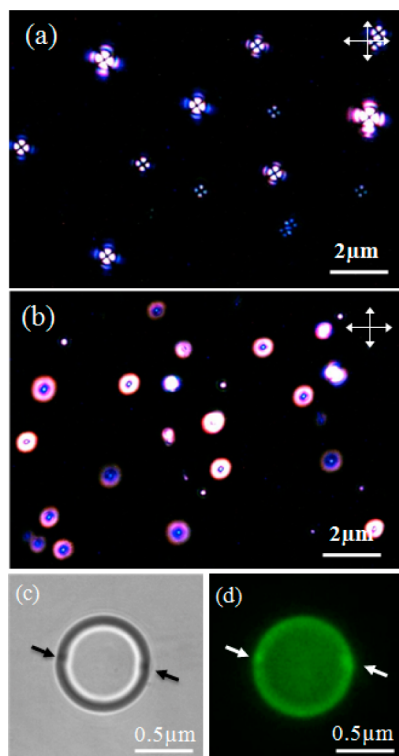


Figure 3. Polarizing optical microscopy images of PDADMAC-modified 5CB droplets in aqueous solution with 150 mM NaCl at pH 7.4 before (a) and after (b) addition of 2 mg/mL BSA. The direction of the polarizer and analyzer is indicated by white arrows in panels a and b. Bright-field (c) and fluorescent (d) images of a PDADMAC-modified 5CB droplet in aqueous solution with 150 mM NaCl at pH 7.4 after addition of 2 mg/mL FITC-labeled BSA. The defect points of the droplet are indicated by arrows in panels c and d.

droplet surface (Figure 3d), suggesting that FITC-BSA is more concentrated at the defect points. The defect point of LC droplets is known to be the disordered region of LC orientation. The localization of the adsorbed spherical polystyrene colloids at the point defects of the LC droplets has been also reported in the literature.³⁴

It has been demonstrated that the formation of an electrical double layer at the 5CB/aqueous interface after addition of NaCl in the aqueous phase can generate an electric field in the diffuse ion region of the double layer that is perpendicular to the interface. The electric field is able to exert a sufficient torque to achieve the homeotropic anchoring of the 5CB at the interface as the increase of NaCl concentrations.³³ The adsorption of BSA on the PDADMAC-modified 5CB droplets leads to the overlap of electrical double layers at the BSA surface and the droplet surface. Thus, the initially formed electrical double layer at the surface of the PDADMAC modified-5CB droplets is disrupted by the adsorption of BSA, leading to the radial-to-bipolar transition of the 5CB inside the droplets.

The configuration transition of PDADMAC-modified 5CB droplets provides an optical probe to detect their interactions with BSA. We find that the concentration of BSA required to induce the radial-to-bipolar transition of the 5CB inside the droplets increases with the decrease of PDADMAC molecular weights. In our experiments, the 5CB droplets modified with PDADMAC having different molecular weights were exposed to 150 mM NaCl aqueous solution at pH 7.4, followed by the addition of BSA at different concentrations. For the 450 kDa PDADMAC-modified 5CB droplets, we find that there is no configuration transition for the 5CB droplets when the concentration of BSA is below 10 $\mu\text{g/mL}$ for a constant adsorption time (30 min). However, all of them become the bipolar configuration when the BSA concentration is above 40 $\mu\text{g/mL}$. In the range from 10 $\mu\text{g/mL}$ to 30 $\mu\text{g/mL}$, the bipolar

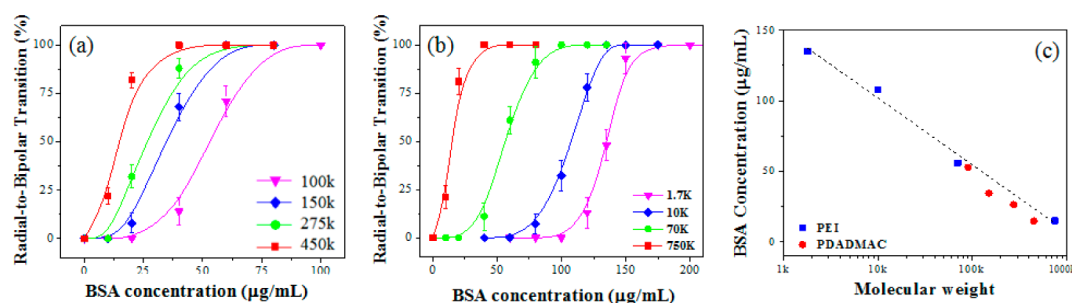


Figure 4. The radial-to-bipolar transition percentage of PDADMAC- (a) and PEI-modified (b) 5CB droplets as a function of BSA concentrations. (c) BSA concentration required to trigger 50% transition of PDADMAC and PEI-modified 5CB droplets as a function of molecular weights. The data points shown in panels a and b were obtained from the statistical result of 100 droplets from each sample.

and radial droplets coexist. The percentage of the bipolar droplets increases rapidly as the increase of BSA concentrations, showing a S-shaped transition curve (Figure 4a). The S-shaped transition curves gradually shift to right with the decrease of the molecular weight of PDADMAC. Figure 4b shows the S-shaped transition curves of PEI-modified SCB droplets in response to the adsorption of BSA in 150 mM NaCl solution at pH 7.4 for 30 min. Again, the S-shaped transition curves gradually shift to right with the decrease of the molecular weight of PEI. For the 750 kDa PEI-modified SCB droplets, 40 $\mu\text{g/mL}$ of BSA is required to achieve 100% of the radial-to-bipolar transition. However, it takes more than 125 $\mu\text{g/mL}$ of BSA to initiate the radial-to-bipolar transition for the 1.7 kDa PEI-modified SCB droplets. For the comparison, we plot the concentration of BSA required to induce 50% of the radial-to-bipolar transition of PDADMAC and PEI-modified SCB droplets as a function of their molecular weights and find that the concentration linearly increases with decreasing the molecular weight of PDADMAC and PEI, respectively (Figure 4c). There is no significant difference observed when the pH is increased from 7.4 to 8.7. It is known that the number of charged groups of PEI and PDADMAC increases with the increase of their molecular weights. The concentration dependence on the molecular weights suggests that electrostatic interaction is responsive for the adsorption of BSA on the PDADMAC and PEI-modified SCB droplets. The linear relationship suggests that the sensitivity of polyelectrolyte-modified SCB droplets for detecting the binding of BSA can be linearly tuned by the molecular weight of polyelectrolytes.

Furthermore, we detect the binding of BSA on PDADMAC- and PEI-modified SCB droplets in PBS solution at pH 7.4 to mimic biological environments. Figure 5a shows the polarizing microscopy image of 750 kDa PEI-SCB droplets in PBS solution. It is clear that PEI-modified SCB droplets transit into a radial configuration. After the addition of 10 $\mu\text{g/mL}$ BSA, some of the PEI-modified SCB droplets transit into bipolar (Figure 5b). When the concentration of BSA reaches 40 $\mu\text{g/mL}$, all of the PEI-modified SCB droplets become bipolar (Figure 5c). The transition curves of 750 kDa PEI and 450 kDa PDADMAC-modified SCB droplets in response to the binding of BSA in PBS solution, together with their transition curves in 150 mM NaCl solution, are shown in Figure 6a, in which BSA with different concentrations was incubated with these SCB droplets for 30 min. The concentration of BSA in PBS solution required to induce 50% the radial-to-bipolar transition is 17 $\mu\text{g/mL}$ for the PDADMAC-modified SCB droplets and 24 $\mu\text{g/mL}$ for the PEI-modified SCB droplets, respectively (Figure 6b). They are close to the concentration of BSA required to induce 50% of the radial-to-bipolar transition of PDADMAC and PEI-modified SCB droplets in 150 mM NaCl solution.

Finally, we exploit the possibility of using the configuration transition of the SCB inside the 750 kDa PEI-modified droplets to detect the adsorption of tobacco mosaic virus (TMV). The adsorption of TMV on 750 kDa PEI-modified SCB droplets through electrostatic interaction can also induce the radial-to-bipolar transition of the SCB inside the droplets. Figure 7 shows the transition curve of 750 kDa PEI-modified SCB droplets after being exposed to TMV at different concentrations in 150 mM NaCl solution at pH 7.4. The radial-to-bipolar transition of PEI-modified SCB droplets occurs at a much higher concentration of TMV, compared to BSA. For example, 40 $\mu\text{g/mL}$ of BSA is sufficient to induce 100% of the transition, whereas 100 $\mu\text{g/mL}$ of TMV only initiates the

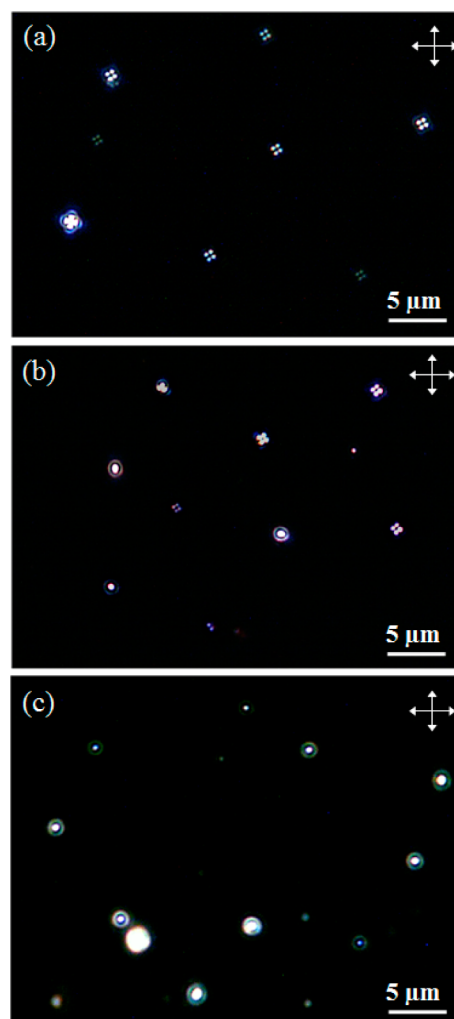


Figure 5. Polarizing optical microscopy images of PEI-modified SCB droplets in PBS solution containing 0.0 $\mu\text{g/mL}$ (a), 10 $\mu\text{g/mL}$ (b), and 60 $\mu\text{g/mL}$ (c) BSA. The direction of the polarizer and analyzer is indicated by white arrows. 750 kDa PEI was used.

transition. At pH 7.4, TMV is negatively charged with a ζ -potential of -30.6 mV, which is higher than that of BSA (-24.5 mV). We know that BSA has an oblate ellipsoid shape with dimensions of $14\text{ nm} \times 4\text{ nm}$. TMV, on the other hand, has a cylindrical shape with 300 nm in length and 18 nm in diameter. It is likely that the adsorption TMV on PEI-modified SCB droplets through electrostatic interaction is hindered by its shape, leading to the increased concentration required to induce the radial-to-bipolar transition of PEI-modified SCB droplets.

In conclusion, we modify the surface of SCB droplets dispersed in deionized water by the adsorption of positively charged PDADMAC and PEI with different molecular weights at the SCB/water interface. The bipolar configuration of PDADMAC and PEI-modified SCB droplets transits into a radial configuration in 150 mM NaCl solution and PBS solution due to the formation of an electrical double-layer at the SCB/aqueous interface. Our results show that the binding of BSA on PDADMAC and PEI-modified SCB droplets by electrostatic interaction can trigger the radial-to-bipolar configuration transition of the SCB inside the droplets, providing a simple optical probe for sensing the binding event. The concentration of BSA required to induce the

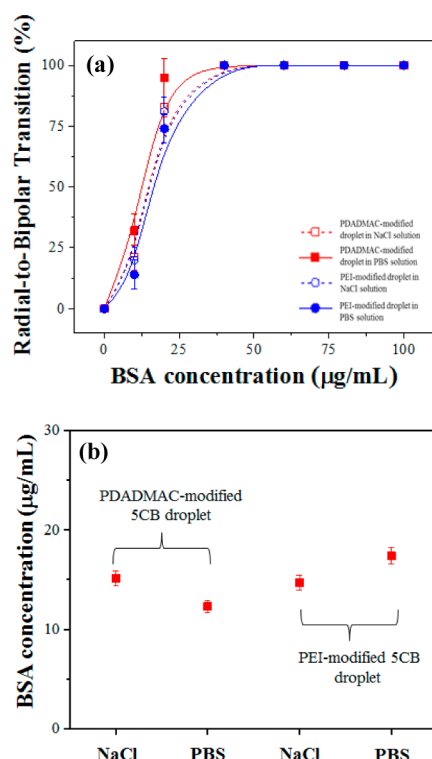


Figure 6. (a) The radial-to-bipolar transition percentage of PDADMAC and PEI-modified 5CB droplets in 150 mM NaCl and PBS solutions at pH 7.4 as a function of BSA concentrations. (c) BSA concentration required to trigger 50% transition of PDADMAC and PEI-modified 5CB droplets. 450 kDa PDADMAC and 750 kDa PEI were used. The data points shown in panel a were obtained from the statistical result of 100 droplets from each sample.

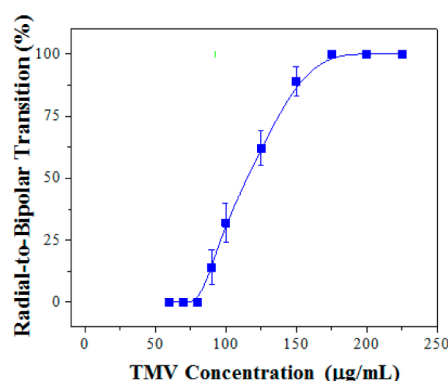


Figure 7. The radial-to-bipolar transition percentage of PEI-modified 5CB droplets in PBS solutions at pH 7.4 as a function of TMV concentrations. PEI with an average molecular weight of 750 kDa was used. The data points were obtained from the statistical result of 100 droplets from each sample.

configuration transition is found to be linearly increase with the decrease of the molecular weight of PDADMAC and PEI. Our results highlight the possibility of using the director configuration of LC droplets as an optical probe for the detection of the interaction of proteins/viruses with polyelectrolytes at the LC/aqueous interface.

AUTHOR INFORMATION

Corresponding Author

*E-mail: Jiyu.Fang@ucf.edu.

Notes

The authors declare no competing financial interest.

ACKNOWLEDGMENTS

This work was supported by the US National Science Foundation (CBET-1264355).

REFERENCES

- (1) Xu, Y.; Mazzawi, M.; Chen, K.; Sun, L.; Dubin, P. L. Protein Purification by Polyelectrolyte Coacervation: Influence of Protein Charge Anisotropy on Selectivity. *Biomacromolecules* **2011**, *12*, 1512–1522.
- (2) Wang, S.; Chen, K.; Xu, Y.; Yu, X.; Wang, W.; Lia, L.; Guo, X. Protein Immobilization and Separation Using Anionic/Cationic Spherical Polyelectrolyte Brushes Based on Charge Anisotropy. *Soft Matter* **2013**, *9*, 11276–11287.
- (3) Caruso, F.; Möhwald, H. Protein Multilayer Formation on Colloids through a Stepwise Self-Assembly Technique. *J. Am. Chem. Soc.* **1999**, *121*, 6039–6046.
- (4) Mohanta, V.; Madras, G.; S. Patil, S. Layer-by-Layer Assembled Thin Film of Albumin Nanoparticles for Delivery of Doxorubicin. *J. Phys. Chem. C* **2012**, *116*, 5333–5341.
- (5) Caruso, F.; Niikura, K.; Furlong, D. N.; Okahata, Y. Assembly of Alternating Polyelectrolyte and Protein Multilayer Films for Immunosensing. *Langmuir* **1997**, *13*, 3427–3433.
- (6) Mallardi, A.; Giustini, M.; Lopez, F.; Dezi, M.; Venturoli, G.; Palazzo, G. Functionality of Photosynthetic Reaction Centers in Polyelectrolyte Multilayers: Toward an Herbicide Biosensor. *J. Phys. Chem. B* **2007**, *111*, 3304–3314.
- (7) Derveaux, S.; Stubbe, B. G.; Roelant, C.; Leblans, M.; De Geest, B. G.; Demeester, J.; De Smedt, S. C. Layer-by-Layer Coated Digitally Encoded Microcarriers for Quantification of Proteins in Serum and Plasma. *Anal. Chem.* **2008**, *80*, 85–94.
- (8) Turgeon, S. T.; Beaulieu, M.; Schmitt, C.; Sanchez, C. Protein–Polysaccharide Interactions: Phase-Ordering Kinetics, Thermodynamic and Structural Aspects. *Curr. Opin. Colloid Interface Sci.* **2003**, *8*, 401–414.
- (9) Saloum, D. S.; Schlenhoff, J. Protein Adsorption Modalities on Polyelectrolyte Multilayers. *Biomacromolecules* **2004**, *5*, 1089–1096.
- (10) Wittemann, A.; Ballauff, M. Interaction of Proteins with Linear Polyelectrolytes and Spherical polyelectrolyte Brushes in Aqueous Solution. *Phys. Chem. Chem. Phys.* **2006**, *8*, 5269–5275.
- (11) Kayitmazer, B.; Seeman, D.; Baykal, B.; Dubin, P. L.; Xu, Y. Protein–Polyelectrolyte Interactions. *Soft Matter* **2013**, *9*, 2553–2583.
- (12) Kusumo, A.; Bombalski, L.; Lin, Q.; Matyjaszewski, K.; Schneider, J. W.; Tilton, R. D. High Capacity, Charge-Selective Protein Uptake by Polyelectrolyte Brushes. *Langmuir* **2007**, *23*, 4448–4454.
- (13) Vaisocherová, H.; Yang, W.; Zhang, Z.; Cao, Z.; Cheng, G.; Piliarik, M.; Homola, J. I.; Jiang, S. Ultralow Fouling and Functionalizable Surface Chemistry Based on a Zwitterionic Polymer Enabling Sensitive and Specific Protein Detection in Undiluted Blood Plasma. *Anal. Chem.* **2008**, *80*, 7894–7901.
- (14) Uto, K.; Yamamoto, K.; Kishimoto, N.; Muraoka, M.; Aoyagi, T.; Yamashita, I. Electrostatic Adsorption of Ferritin, Proteins and Nanoparticle Conjugate onto the Surface of Polyelectrolyte Multilayers. *J. Mater. Chem.* **2008**, *18*, 3876–3884.
- (15) Gormally, C. M. V.; McKibben, R. K.; Johal, M. S.; Selassie, C. R. D. Controlling Tyrosinase Activity on Charged Polyelectrolyte Surfaces: A QCM-D Analysis. *Langmuir* **2009**, *25*, 10014–10019.
- (16) Kepplinger, C.; Lisdat, F.; Wollenberger, U. Cytochrome c/ Polyelectrolyte Multilayers Investigated by E-QCM-D: Effect of Temperature on the Assembly Structure. *Langmuir* **2011**, *27*, 8309–8315.
- (17) Kreft, O.; Prevot, M.; Möhwald, H.; Sukhorukov, G. B. Shell-in-Shell Microcapsules: A Novel Tool for Integrated, Spatially Confined Enzymatic Reactions. *Angew. Chem., Int. Ed.* **2007**, *46*, 5605–5608.

- (18) Miao, Y. H.; Helseth, L. F. Adsorption of Bovine Serum Albumin on Polyelectrolyte-Coated Glass Substrates: Applications to Colloidal Lithography. *Colloids Surf., B* **2008**, *66*, 299–303.
- (19) She, Z.; Antipina, M. N.; Li, J.; Sukhorukov, G. B. Mechanism of Protein Release from Polyelectrolyte Multilayer Microcapsules. *Biomacromolecules* **2010**, *11*, 1241–1247.
- (20) Carlton, R. J.; Hunter, J. T.; Miller, D. S.; Abbasi, R.; Mushenheim, P. C.; Tan, L. N.; Abbott, N. L. Chemical and Biological Sensing using Liquid Crystals. *Liq. Cryst. Rev.* **2013**, *1*, 29–51.
- (21) Volovik, G. E.; Lavrentovich, O. D. Topological Dynamics of Defects: Boojums in Nematic Drops. *Sov. Phys. JETP* **1983**, *58*, 1159–1167.
- (22) Hsu, P.; Poulin, P.; Weitz, D. A. Rotational Diffusion of Monodisperse Liquid Crystal Droplets. *J. Colloid Interface Sci.* **1998**, *200*, 182–184.
- (23) Tjipito, E.; Cadwell, K. D.; Quinn, J. F.; Johnston, A. P. R.; Caruso, F.; Abbott, N. L. Tailoring the Interfaces between Nematic Liquid Crystal Emulsions and Aqueous Phases via Layer-by-Layer Assembly. *Nano Lett.* **2006**, *6*, 2243–2248.
- (24) Kinsinger, M. L.; Buck, M. E.; Abbott, N. L.; Lynn, D. M. Immobilization of Polymer-Decorated Liquid Crystal Droplets on Chemically Tailored Surfaces. *Langmuir* **2010**, *26*, 10234–10242.
- (25) Zou, J.; Fang, J. Y. Director configuration of liquid-crystal droplets encapsulated by polyelectrolytes. *Langmuir* **2010**, *18*, 7025–7028.
- (26) Zou, J.; Bera, T.; Davis, A. A.; Liang, W.; Fang, J. Y. Director Configuration Transitions of Polyelectrolyte Coated Liquid-Crystal Droplets. *J. Phys. Chem. B* **2011**, *115*, 8970–8974.
- (27) Aliño, V. J.; Pang, J.; Yang, K. L. Liquid Crystal Droplets as a Hosting and Sensing Platform for Developing Immunoassays. *Langmuir* **2011**, *27*, 11784–11789.
- (28) Khan, W.; Choi, J. H.; Kim, G. M.; Park, S. Y. Microfluidic Formation of pH Responsive SCB Droplets Decorated with PAA-b-LCP. *Lab on a Chip*. **2011**, *11*, 3493–3498.
- (29) Bera, T.; Fang, J. Y. Polyelectrolyte-Coated Liquid Crystal Droplets for Detecting Charged Macromolecules. *J. Mater. Chem.* **2012**, *22*, 6807–6812.
- (30) Aliño, V. J.; Sim, P. H.; Choy, W. T.; Fraser, A.; Yang, K. Y. Detecting Proteins in Microfluidic Channels Decorated with Liquid Crystal Sensing Dots. *Langmuir* **2012**, *28*, 17571–17577.
- (31) Manna, U.; Zayas-Gonzalez, Y. M.; Carlton, R. J.; Caruso, F.; Abbott, N. L.; Lynn, D. M. Liquid Crystal Chemical Sensors that Cells Can Wear. *Angew. Chem., Int. Ed.* **2013**, *52*, 14011–14015.
- (32) Kim, J.; Khan, M.; Park, S. Y. Glucose Sensor Using Liquid-Crystal Droplets Made by Microfluidics. *ACS Appl. Mater. Interfaces* **2013**, *5*, 13135–13139.
- (33) Carlton, R. J.; Gupta, J. K.; Swift, C. L.; Abbott, N. L. Influence of Simple Electrolytes on the Orientational Ordering of Thermotropic Liquid Crystals at Aqueous Interfaces. *Langmuir* **2012**, *28*, 31–36.
- (34) Mondiot, F.; Wang, X.; de Pablo, J. J.; Abbott, N. L. Liquid Crystal-Based Emulsions for Synthesis of Spherical and Non-Spherical Particles with Chemical Patches. *J. Am. Chem. Soc.* **2013**, *135*, 9972–9975.